

FIG. 1. Ratios for NaF, Li^7F , and NaI of $v_{\text{II}}(T)$, the computed velocity of second sound at temperature T to $v_{\text{II}}(0)$, the value at $T=0^\circ\text{K}$ vs T/Θ_D , where Θ_D is the Debye temperature. The arrow indicates the temperature at which $v_{\text{II}}(T)$ for NaF is the same as the velocity of the observed second-sound pulses (see Ref. 1).

J_3 was used). The sound velocities for the different directions and polarizations which were needed were calculated from the elastic constants C_{11} , C_{12} , C_{44} and the densities ρ given in Table I. The 0°K

values of the Debye temperature Θ_D given in Table I were determined with Eq. (3.2) of Betts, Bhatia, and Wyman.⁷ [Note that the J in their Eq. (3.2) is the same as our $4\pi \langle v_s^3 \rangle$.]

The velocity of second sound decreases with increasing temperature because of the dispersion in the phonon frequency spectrum. The effect is particularly significant in NaI. To illustrate this, the ratio of the velocity of second sound at temperature T to its 0°K limiting value is plotted as a function of temperature in Fig. 1. Ratios are given for NaI, Li^7F , and NaF. The numbers for NaF are from Ref. 1. The temperature axis is scaled for the different materials according to the values of Θ_D given in Table I. The arrow in Fig. 1 indicates the approximate temperature (18°K) at which the velocity of the second-sound pulses observed in NaF was the same as the computed value.⁸ Note that v_{II} for NaF at 18°K is 6.6% smaller than its 0°K value, while v_{II} for NaI at the same value of T/Θ_D ($T=6^\circ\text{K}$) is 19% less than its 0°K value. The very dispersive nature of the frequency spectrum of NaI is also apparent from the values of C_0/T^3 given in the tables. Deviations from proportionality to T^3 in the temperature dependence of C_0 at low temperatures (below about $\Theta_D/20$) are due to the dispersion in the frequency spectrum.

¹R. J. Hardy and S. S. Jaswal, Phys. Rev. B **3**, 4385 (1971).

²H. E. Jackson, C. T. Walker, and T. F. McNelly, Phys. Rev. Letters **25**, 26 (1970); H. E. Jackson and C. T. Walker, Phys. Rev. B **3**, 1428 (1971).

³T. F. McNelly, S. J. Rogers, D. J. Channin, R. J. Rollefson, W. M. Goubau, G. E. Schmidt, J. A. Krumhansl, and R. O. Pohl, Phys. Rev. Letters **24**, 100 (1970); S. J. Rogers, Phys. Rev. B **3**, 1440 (1971).

⁴S. S. Jaswal and J. R. Hardy, Phys. Rev. **171**, 1090 (1968).

⁵R. P. Lowndes and D. H. Martin, Proc. Roy. Soc.

(London) **A308**, 473 (1969).

⁶G. Dolling, H. G. Smith, R. M. Nicklow, P. R. Vijayaraghavan, and M. K. Wilkinson, Phys. Rev. **168**, 970 (1968).

⁷D. D. Betts, A. B. Bhatia, and M. Wyman, Phys. Rev. **104**, 37 (1956).

⁸Distinct second-sound pulses were not observed above 18°K in NaF. Apparently there is not sufficient normal-process scattering below 18°K for the damped-wave equation, which predicts v_{II} for the velocity of a second-sound pulse, to be strictly valid for NaF. See Ref. 1.

Compton Profile of Polycrystalline Lithium

Walter C. Phillips*

Physics Department, Brandeis University, Waltham, Massachusetts 02154

and

R. J. Weiss

Army Materials and Mechanics Research Agency, Watertown, Massachusetts 02172

(Received 9 August 1971)

The Compton profile of polycrystalline Li has been remeasured and is compared with profiles predicted by recent calculations of the Li-electron-momentum distribution.

Measurements of Compton scattering from polycrystalline Li were made with considerably better

instrumental resolution and smaller statistical uncertainty than our previous Li measurements, and

thus a more accurate assessment of the magnitude of x-ray scattering (electron momenta), particularly above the Fermi momentum, can be made.¹ Our results and the recent experimental results of Cooper, Williams, Borland, and Cooper are in excellent agreement.² Compton profiles predicted by current band calculations differ from the measurements by about 8% at $J(0)$.

The apparatus is similar to that previously described¹: with the significant differences of a large Li polycrystalline sample (3.6-cm beam path) with no impurity lines in the region of interest, a $\pm 3^\circ$ (maximum divergence) Soller-slit collimator on the Mo-target x-ray tube, a Compton scattering angle $2\theta_c = 158^\circ$, a LiF analyzing-crystal (800) reflection, and a more stable data-acquisition system. Some 800 scans over the Compton line at LiF 2θ intervals of $0.04^\circ \approx 0.00023 \text{ \AA} \approx 0.022 \text{ a.u.}$ (atomic units of electron momentum) were added to give over 10^5 x rays per data point in the center region of the profile.

For a polycrystalline sample the Compton profile $J(z)$ and the one-electron ground-state momentum-wave function $\chi_i(\vec{p})$ are related in the impulse approximation by the expression

$$J(z) = \sum_i 2\pi \int_{|z|}^{\infty} |\chi_i(p)|^2 p dp, \quad (1)$$

where $|\chi_i(p)|^2$ is the spherically averaged momentum density and z is the electron-momentum component along the scattering vector:

$$z = \frac{mc}{2\lambda_0 \sin\theta_c} \left(\lambda - \lambda_0 - \frac{2h}{mc} \sin^2\theta_c \right)$$

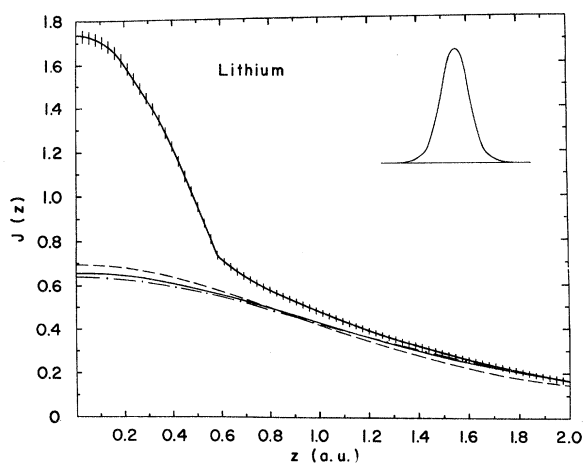


FIG. 1. Experimentally determined Li Compton profile folded about $z=0$ and averaged (solid line). The estimated experimental uncertainty is shown by the vertical lines. Curves I (solid line), II (dashed line), and III (dot-dashed line) are the calculated $1s^2$ (core) profiles described in the text. The instrumental-resolution function is shown in the inset.

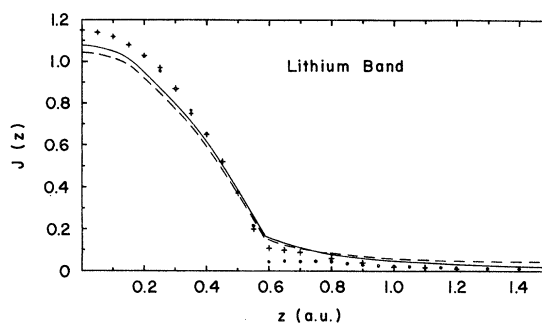


FIG. 2. Compton profiles for the Li band. Curves I (solid line) and II (dashed line) are obtained from the experimental profile in Fig. 1 by subtracting the corresponding calculated-core profiles. The profiles derived from band calculations of Borland and Cooper (closed circles) and Lundqvist and Lydén (crosses) predict $J(z)$ values somewhat higher near $z=0$ and lower at large z .

$$\times \left[1 + \frac{\lambda - \lambda_0}{\lambda_0} + \left(\frac{\lambda - \lambda_0}{2\lambda_0 \sin\theta_c} \right)^2 \right]^{-1/2}, \quad (2)$$

where λ_0 is the wavelength of the incident x ray ($\text{Mo}K\alpha_1 = 0.70930 \text{ \AA}$) and λ is the wavelength of the scattered x-ray. Eisenberger and Platzman³ have shown that the impulse approximation is valid to terms of order $[E_B/E_R(\lambda)]^2$, where E_B is the binding energy and $E_R(\lambda)$ is the electron-recoil energy. [For our experimental conditions for the range of momenta shown in the figures, we have $E_R > 620 \text{ eV}$, and since $E_B(1s) = 55 \text{ eV}$ in Li, then $(E_B/E_R)^2 < 0.008$.] The same authors find excellent agreement in He between the measured Compton profile and a free-atom calculation using Eq. (1). Currat, DeCicco, and Weiss have also recently provided justification for using the impulse approximation for accurate calculations of Compton profiles of low- Z elements.⁴

The experimental Li Compton profile, folded about the centroid ($z=0.00$) and averaged, is shown in Fig. 1. To arrive at this curve the data (intensity vs LiF 2θ) are analyzed in the following way: A smooth curve is drawn through the data, and the background, primarily Compton scattering of the bremsstrahlung, is subtracted ($K\alpha$ Compton/background ~ 6.5 at $z=0$). A linear correction to the measured intensity for various wavelength-dependent terms is then made. [For these data the final $J(z)$ is not significantly altered if this correction is omitted.] The $\text{Mo}K\alpha_1$ and $\text{Mo}K\alpha_2$ components of the scattering are separated using the Rachinger method, and the effects of instrumental broadening, relatively important only near the Fermi momentum p_F , are effectively removed by an iterative procedure. [The instrumental resolution, full width at half-maximum (FWHM) = 0.134 a.u. , is shown in Fig. 1.] The resulting curve is converted to an

TABLE I. Lithium Compton profiles. The total experimental uncertainty in $J(z)$ is $\sim \pm 0.02$ for all entries.

z	Total $J(z)$	Experiment		Calculated	
		Curve I band $J(z)$	Curve II band $J(z)$	Ref. 6 band $J(z)$	Ref. 7 band $J(z)$
0.00	1.73	1.08	1.04	1.15	1.15
0.05	1.72	1.07	1.03	1.14	1.14
0.10	1.70	1.05	1.02	1.12	1.12
0.15	1.66	1.01	0.98	1.08	1.08
0.20	1.60	0.95	0.92	1.02	1.03
0.25	1.51	0.87	0.85	0.95	0.97
0.30	1.43	0.80	0.77	0.87	0.87
0.35	1.34	0.72	0.69	0.77	0.75
0.40	1.22	0.62	0.59	0.65	0.65
0.45	1.10	0.50	0.48	0.52	0.52
0.50	0.97	0.38	0.36	0.37	0.37
0.55	0.83	0.26	0.24	0.21	0.20
0.60	0.72	0.16	0.15	0.04	0.11
0.65	0.67	0.13	0.12	0.05	0.10
0.70	0.64	0.11	0.11	0.05	0.09
0.80	0.58	0.08	0.08	0.05	0.06
0.90	0.52	0.06	0.07	0.03	0.04
1.00	0.48	0.05	0.06	0.02	0.02
1.10	0.43	0.04	0.05	0.02	0.02
1.20	0.39	0.03	0.05	0.01	0.01
1.30	0.35	0.02	0.04	0.01	0.00
1.40	0.32	0.02	0.04	0.01	
1.50	0.29	0.02	0.04	0.01	
1.60	0.26	0.01	0.04	0.01	
1.70	0.23	0.01	0.04	0.01	
1.80	0.21	0.01	0.03	0.01	
1.90	0.18	0.01	0.02	0.01	
2.00	0.16	0.00	0.02	0.01	

electron-momentum (z) scale and the area is normalized. Over the range of z shown in Fig. 1, the $J(z)$ curves for $z > 0$ and $z < 0$ agree with the experimental uncertainty.

Since the Compton measurement is not an absolute one, the experimentally determined $J(z)$ must be scaled. This is accomplished by adjusting the height so that the area under some region $0 \leq z \leq z_m$ corresponds to the expected number of electrons. For $J(z)$ in Fig. 1,

$$\int_0^{2.00} J(z) dz = 0.500 \text{ band electrons} \\ + 0.847 \text{ core electrons}$$

(corresponding to the free-atom core calculation below). $J(z)$ is not significantly changed if $z_m = 2.5$ or 3.0 a. u. Because the $K\alpha$ Compton/background scattering in Li is small for large z , the accuracy of the normalization is not improved for $z_m \gtrsim 2.0$

*Research supported by National Science Foundation Grant No. GU 3852.

¹W. C. Phillips and R. J. Weiss, Phys. Rev. **171**, 790 (1968).

²M. Cooper, B. G. Williams, R. E. Borland, and J. R. A. Cooper, Phil. Mag. **22**, 441 (1970).

³P. Eisenberger and P. M. Platzman, Phys. Rev. A **2**, 415 (1970).

⁴R. Currat, P. D. DeCicco, and R. J. Weiss, Phys. Rev. (to be published); and P. D. DeCicco (private com-

munication).

Three calculated $1s^2$ profiles are shown in Fig. 1. Curve I is an impulse-approximation calculation for a Clementi-Hartree-Fock Li^+ free-atom wave function [$\int_0^{2.00} J_I(z) dz = 0.847$].⁵ Curve II is the Borland and Cooper impulse-approximation core calculated for the self-consistent wave function they derive using a Seitz potential and a basis set consisting of tight-binding Bloch orbitals (core) and plane waves (band) [$\int_0^{2.00} J_{II}(z) dz = 0.853$].⁶ Curve III is a calculation by DeCicco in which the $1s^2$ profile is calculated in the Born approximation by employing excited-state one-electron continuum wave functions evaluated in the ground-state Hartree-Fock-Slater potential of the nucleus and remaining electrons.⁴ The DeCicco result has been shifted + 0.04 a. u. in order to obtain a profile symmetric about $z = 0$ [$\int_0^{2.00} J_{III}(z) dz = 0.830$]. Clearly there is close agreement between this calculation and the free-atom impulse approximation (curve I), as noted in Ref. 4.

"Band" profiles, obtained by subtracting curves I and II from the experimental $J(z)$, are shown in Fig. 2. Calculations of the band profile by Borland and Cooper, and by Lundqvist and Lydén (averaged over the three crystallographic directions they derive), are also shown.^{6,7} Numerical values for all curves are given in Table I. The calculation in Ref. 7 is an orthogonalized-plane-wave calculation in which the effects of the orthogonalization of band and core, the periodic potential, and correlation are considered. To the extent that the core calculations accurately describe the $1s^2$ electrons in the solid, the calculated-band profiles are seen to differ significantly from the experimental profile; there is more measured momentum density at higher momenta and a corresponding depression at $J(0)$. Cooper *et al.* have found the same discrepancy between their Li Compton measurement and band calculation.² Even larger discrepancies occur for other calculations.⁸ Whether the difference between the experiment and calculations is due to inadequacies in the band or the core calculations is, at present, undetermined. It seems most likely that the tail above p_F is due to electron-electron correlations. There is some question as to the meaning of making a separation of the three Li electrons into two core electrons and one band electron.

munication).

⁵R. J. Weiss, A. Harvey, and W. C. Phillips, Phil. Mag. **17**, 241 (1968).

⁶R. E. Borland and J. A. R. Cooper, J. Phys. C Suppl. **3**, S253 (1970).

⁷B. I. Lundqvist and C. Lydén, Phys. Rev. (to be published).

⁸D. J. W. Geldart, A. Houghton, and S. H. Vosko, Can. J. Phys. **42**, 1938 (1964); and J. Lam, Phys. Rev. B **3**, 3243 (1971).